Analysis and Study of a Mesoscale Inertia–Gravitational Wave in Upper Air

Zhang Ying (张颖), *Shen Xinyong* (沈新勇)
and *Zhang Ming* (张铭)①
Laboratory for Numerical Modeling of Atmospheric Sciences and Geophysical Fluid Dynamics, Academia Sinica, Beijing, 100080
Received January 23, 1989

ABSTRACT

A mesoscale inertia–gravitational wave at 200 hPa is analysed. The reasons of this wave occurring are also discussed. It is indicated that the occurrence of this wave is due to inertia–gravitational instability, and closely related to horizontal and vertical shear of wind.

I. INTRODUCTION

Inertia–gravitational wave is of great importance in the atmosphere. Mesoscale and microscale inertia–gravitational waves are increasingly paid attention to at present. Its major characteristics are summarized at Table 39 in reference (B. W. Atkinson, 1987). Because of limited observation method, at upper troposphere the observation of inertia–gravitational wave which has rather longer length is much fewer. In fact, it is usually inertia–gravitational wave's generation area where its instability exists in the result of intensive horizontal and vertical shear of stream field near the jet at upper troposphere (Zeng Qingcun, 1977 and Zhang Kesu, 1988). And an unstable inertia–gravitational wave is usually companied with intense air turbulence in the same area.

During "Mesoscale Weather Experiment in East China" radiosonde observation was intensified in space and time, so this has contributed to discover mesoscale inertia–gravitational wave at upper troposphere. And we really find out that there is an inertia–gravitational wave at upper troposphere.

II. METHOD OF DATA ANALYSIS

In this paper, the data we used are intensive one at 12 GMT on 27 April, 1983 during "Mesoscale Weather Experiment in East China", in addition to the data in "Meteorological Monthly Report in Upper Air". It has altogether 24 radiosonde stations. Our main works include direct plotting and drawing of four mandatory surface at 300, 250, 200 and 100 hPa, obtaining of grid point data and filter analysis. We design a 15 × 15 grid mesh from 29.2°N to 34.9°N, 114.9°E to 122.6°E, and the mesh distance is equal. The method to filter fast wave proposed by Zeng Qingcun is adopted in order to emphasize mesoscale disturbance. As to any physical variable, F, for instance, can be separated into $\bar{F}$ and F', i.e. $F=\bar{F}+F'$, where $\bar{F}$ is slow process in the atmosphere, and F' is part of fast wave

①Project supported by the National Science Foundation of China

(inertia–gravitational wave for example). If scale separation is done by using this method, mesoscale distrubance will be emphasized and large scale field will be uniformly smoothed. From many trials it is indicated that such a filter method is very effective.

III. CHARACTERISTICS OF LARGE–SCALE CIRCULATION FIELD

At 200 hPa, the situation is typical of one trough and one ridge for 12 GMT on 27 April, 1983. There is a cold vortex in the vicinity of 130°E, 65°N. And the trough line is close to 125°E, which extends from the center of the vortex low to Harbin, Shenyang, Seoul and Okinawa. From 50°E to 60°E there is a blocking high. From 125°E to 100°E and 27°N to 40°N there exists a jet area and the maximum wind speed is roughly 56 m / s. 125°E eastwards, the jet position is rather north. East China is just under the westerly jet behind the trough.

At 500 hPa, the blocking high is to the west of Ural mountains, and to the east is a trough area. The trough line is located from Harbin, Shenyang to Qingdao. In addition, there is also a small trough existed from Hami to Tibetan Plateau. A high exists in Indo–China, and the jet area located between 38°N and 45°N is somewhat weak. The straining westerly current is just over the experiment area in East China.

At surface, there is a cyclone at north–western Japanese Sea and its cold front is situated from Osaka, Nagasaki, Fuzhou, Guangzhou to Nanning. There is a strong high behind it. The high center is located in the vicinity of Hohhot and the high center is 1031 hPa. Since East China is behind the cold front and ahead of the high, it is under the control of mediocris or high cloud (cirrofilum for instance).

IV. ANALYSIS RESULTS OF ORIGINAL DATA

It is found out from the analysis that there is a clear mesoscale wave at 200 hPa. It can be obviously seen in u and v component fields which are directly plotted on the map, even if no filtering is made. On the distribution chart of u component, there is a series of apparent mesoscale waves from Hongze Lake through to Nanjing. Its wavelength is about 220 kilometers and the maximum amplitude of u exceeds 10 m / s (as shown in Fig. 1), where it is defined the difference between the maximum and minimum value of any physical variables as maximum amplitude, so do afterwards without special illustration. At 200 hPa, there is also a mesoscale wave in v field and the wave also locates from Hongze Lake through to Nanjing as u field does (figure omitted). And the amplitude of mesoscale wave of 200 hPa also exceeds 10 m / s. In addition, it is obvious that the amplitude of mesoscale wave at 200 hPa is the largest one of all, so that the wave at 200 hPa is the clearest. On the contrary, the amplitude above and under 200 hPa is generally getting smaller. Accordingly, the mesoscale wave at 200 hPa is mainly discussed as follows.

At height field of 200 hPa, mesoscale wave is less clear than in wind field because of apparent south high and north low situation in large scale pressure field. On the other hand, the mesoscale wave in wind field is more clear than that in height field.

V. ANALYSIS RESULTS OF FILTERED DATA

After finishing the scale separation, the mesoscale wave would be more clear because the large scale field is filtered.

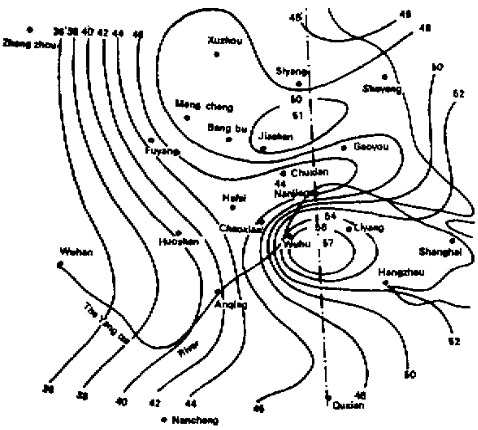

Fig. 1. Distribution of u at 200 hPa, unit of isopleth is ms^{-1} (12 GMT 27 April, 1984).

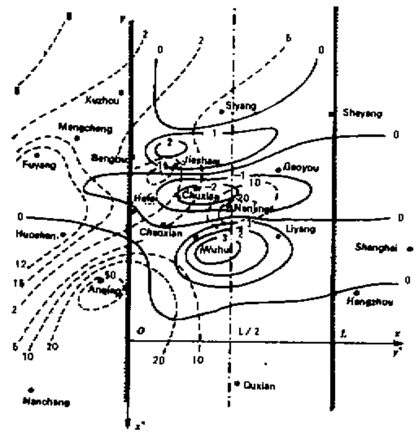

Fig. 2. The field of u (solid line, unit: ms^{-1}) and the distribution of Ri (dashed line) (12 GMT 27 April, 1984).

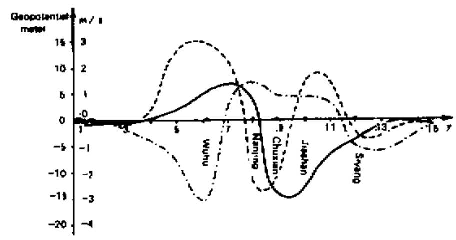

Fig. 3. —— u' —·—·—·— v' —— H' (12 GMT 27 April, 1984).

The field of u at 200 hPa is just shown in Fig. 2. It is obvious that the mesoscale wave is quite clear, and its wave width is roughly 4 grid spacing (180 kilometers).

Apart from this, there are no waves at all. The wave is north–south in direction, the wave–length is about 5 grid spacing (225 kilometers), the maximum amplitude is 5.5 m / s. In the same case, the field of v at 200 hPa is also existed mesoscale wave through filtering and its amplitude is 4.5 m / s. In addition, there is a mesoscale wave in H' field at 200 hPa, but it is not as clear as that in u' or v' field. The distributions of u', v' and H' on north and south cross–section through Nanjing are shown in Fig. 3. From Fig. 3 the relations among them can be clearly seen.

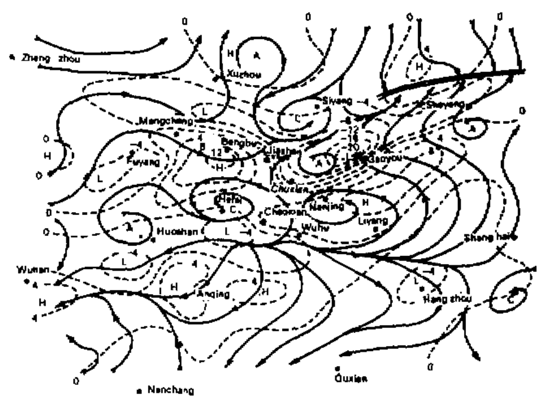

Fig. 4. —— H' , ——disturbed stream field. (12 GMT 27 April, 1984).

As shown in Fig. 4, the disturbance stream field is appropriately accompanied with disturbance height field at 200 hPa in terms of characteristics of inertia–gravitational wave. At 200 hPa, cyclone on disturbance stream field is almost overlapped high on disturbance height field. On the other hand, anticyclone on disturbance stream field is nearly overlapped low on disturbance height field. Such characteristics are just testified the existence of inertia–gravitational wave (Yang Guoxiang, 1983).

VI. DISCUSSIONS AND CONCLUSION

1. *Characteristics of Wave*

We think the mesoscale wave at 200 hPa illustrated above is existed objectively instead of observational error. The characteristics of the wave are inertia–gravitational. Now we try to compare the wave with given model wave as follows.

It is well known that if linearized equations of static equilibrium are made variable separated, the vertical and horizontal structure equations can be then obtained. The latter equations are of the same structure with linearized barotropic primitive equation. Accordingly, if we discuss the horizontal structure of wave illustrated above, we can take the advantage of linearized barotropic primitive equation model.

As shown in Fig. 2, a coordinates system $(0, x^*, y^*)$ is designed. Its x^* axis directs to south, y^* axis directs to east, and every physical quantity in the system is marked "*" to distinguish. So, it is obvious that

$$u^* = -v', \qquad v^* = u'. \tag{1}$$

Thus the distribution of v^* is just the same as u' in Fig. 2. Therefore, in general

$$u'|_{y^*=0} = v^*|_{y^*=0} = 0, \quad u'|_{y^*=L} = v^*|_{y^*=L} = 0. \tag{2}$$

In this case, it can be considered that the wave in Fig. 2 is confined in the passage formed between $y^*=0$ and $y^*=L$. It is also noticed that the wave of v^* has no nodal point in the passage 0–L.

At 200 hPa, in the passage $0\text{–}L$, supposing a barotropic primitive equation model in which f equals a constant, so the Poincare wave mode of inertia–gravitational wave is existed under boundary condition (2). Corresponding with the mode which has no nodal point of v^* in the passage 0–L, we obtain $n=1$. In this case, the following relations can be obtained from (3.9.16) in reference (Joseph Pedlosky, 1979) at $y^* = L/2$, or at south and north cross–section through Nanjing in Fig. 2 (dot–dashed line marked in Fig. 2) that

$$H^* = -AfL\cos(kx^* - \sigma t + \varphi)/(\pi c) \quad (3)$$

$$u^* = -AfL\cos(kx^* - \sigma t + \varphi)/(H_0 \pi) \quad (4)$$

$$v^* = -AL(f^2 + gH_0\pi^2 / L^2)\sin(kx^* - \sigma t + \varphi)/(H_0 \sigma \pi), \quad (5)$$

where A is any amplitude constant. φ is any initial phase constant. c is the wave velocity propagated in north and south direction. If $c>0$, the propagation is toward south. If $c<0$, the wave propagates toward north. In addition, H_0 is the atmospheric scale height. k is the wave number in north and south direction. L is the width of passage, and $\sigma = kc$ is the frequency.

If Eqs. (3), (4) and (5) are transformed into original system when we properly translate coordinate origin into y axis at fixed time t, we can obtain that

$$H' = -AfL\cos(ky)/(\pi c) \quad (6)$$

$$v' = AfL\cos(ky)/(H_0 \pi) \quad (7)$$

$$u' = AL(f^2 + gH_0\pi^2 / L^2)\sin(ky)/(H_0 kc\pi)$$

$$= -AL(f^2 + gH_0\pi^2 / L^2)\cos(kx + \frac{\pi}{2})/(H_0 kc\pi). \quad (8)$$

From the matching relation of H', u' and v' in (6), (7) and (8), it is easy to judge the propagation direction. In (6), (7) and (8), if $f>0$, the phase difference between H' and u' is always $-\pi/2$ (only the case when $f>0$ is discussed here). Differently, the matching relation of H' and v' varies along with the wave propagation direction. If $c>0$, the wave propagation direction is from north to south, H' and v' are out–of–phase. If $c<0$, the wave propagation direction is from south to north, H' and v' are in phase.

Now we compare the wave structure of u', v' and H' field on north and south cross–section through Nanjing after filtering at 200 hPa (Fig. 3) with (6), (7) and (8). As shown in Fig. 3 it is indicated that H' and v' in general are out–of–phase and the phase difference between H' and u' is about $-\pi/2$. So, the discovered mesoscale wave's structure at 200 hPa actually corresponds to Poincare wave mode of inertia–gravitational wave when $n=1$. Meanwhile, the wave propagation direction is from north to south. Certainly, the wave is somewhat different from the ideal mode illustrated above. First, the real wave is not a normal sinusoidal one, but a wave packet instead. Second, in the real wave motion, v' is not at its maximum when H' is at its minimum. This is easy to understand because there are also wave motions outside the passage 0–L when H' gets its minimum. Therefore, the passage is as if widened there. So v' certainly decreases in terms of the principle of continuity. In such a situation, v' is not at its maximum correspondingly while H' is at its minimum.

In conclusion, the mode illustrated above is capable of explaining qualitatively the matching relations among u', v' and H' of mesoscale wave discovered now. In fact, this mesoscale wave is confirmed a kind of inertia–gravitational wave. It is also confirmed that the propagation direction is from north to south.

2. *Dynamic Mechanism of Wave Generation*

At 200 hPa, such an apparent mesoscale inertia–gravitational wave is existed, since there is inertia–gravitational instability there. For example, Zhang Kesu (1988) has studied the mesoscale instability of baroclinic flow and particularly calculated two simple cases, namely symmetric instability and transversal wave instability. According to her calculation, it is shown that the increasing rate of whether symmetric or transversal wave instability is related to Richardson Number Ri. The smaller Ri is, the bigger the increasing rate. For symmetric instability, a criterion of the instability was obtained:

$$Ri < \frac{f}{f_a} - \frac{f_a}{f} n^2 (\frac{L}{L_0})^2, \tag{9}$$

where $f_a = f - \partial u / \partial y$, n can be 1, L is the wavelength and L_0 is the radius of thermal wind inertial circle. If $f_a < 0$, then the wave is inertial unstable. If $f_a > 0$, and $Ri < f / f_a$, then the wave is stable and sometimes symmetric unstable. Therefore, it is obvious that the instability of mesoscale wave at 200 hPa just discussed above is more complicated than the symmetric instability. However, if the passage is unlimited, the situation is just the case of symmetric instability. So it is better to estimate the situation by using (6), (7) and (8).

The case in our study has horizontal wind shear and the horizontal shear reaches its maximum in the vicinity of Jiashan. We take advantage of the data of two stations, Jiashan and Fuyang, to calculate f / f_a. The horizontal wind shear at Jiashan station, for instance, is up to $\partial u / \partial y = 1.25 \times 10^{-4} s^{-1}$. Meanwhile, at the station $f_a = -0.45$, $s < 0$, thus, $f / f_a = -1.8$ and the condition of inertial instability is adequate there. As to Fuyang station, it is inertial stable because $\partial u / \partial y = 0.33 \times 10^{-4} s^{-1}$, $f_a = 0.46 \times 10^{-4} s^{-1} > 0$, and $f / f_a = 1.7$. But if $Ri < f / f_a = 1.7$, it is still symmetric unstable there.

In our study, Richardson number at every station is calculated and its distribution is also plotted in Fig. 2 (dash line is its isopleth). As shown in Fig. 2, Fuyang locates at the area of its $Ri = 1.07 < 1.7$, so that station is symmetric unstable. Apart from this, Jiashan is under inertial instability, then the increasing rate of the wave there is particularly large and the wave is the clearest one. It is well known that Ri and vertical wind shear have good relations with each other. Since the wind difference between 300 hPa and 200 hPa is calculated, it can be seen that the wind difference between the two levels is adequately coincided at the area where the velocity is over 20 m / s and $Ri < 2$ (figure omitted). It is determined from the above estimation that the generation of mesoscale inertia–gravitational wave at 200 hPa is closely related to the horizontal and vertical wind shear. It is the results of the development of unstable inertia–gravitational wave. Its unstable sorts are inertial instability and complete inertia–gravitational wave instability in shear–stratified fluid (symmetric instability is its particular situation also).

Since no intensive radiosonde data are available at this time scale, the wave structure instead of its evolution is mainly discussed in this paper.

At present, most of the aircrafts are capable of aviating at upper troposphere, where clear–air turbulence (CAT) intensely influences the air aviation. Usually CAT is found within a thin layer at upper troposphere and is about 600m in depth, 20 km in width, and about 80 to 160 km in length. CAT's alignment is the same as the direction of air flow. Its scale indicates that CAT's origin is related to the mesoscale structure of the atmosphere. Since CAT mainly happens through the crushing of unstable inertia–gravitational wave, it is closely related to the vertical–wind shear. In our case, because the mesoscale inertia–gravitational wave is quite obvious, it is suggested that CAT perhaps exists, although there are no sufficient data to verify. However, it is of great importance in theory and application to investigate the relationship between mesoscale inertia–gravitational wave and CAT.

REFERENCES

Atkinson, B.W. (1987), Mesoscale Circulation in the Atmosphere, Meteorological Press, pp.297–299.

Pedlosky, Joseph (1979), *Geophysical Fluid Dynamics*, pp. 75–81.

Yang Guoxiang (1983), Mesoscale and Microscale Synoptics, Meteorological Press, pp. 93–99.

Zhang Kesu (1988), Instability of Baroclinic Basic Flow I, *Acta Meteorologica Sinica*, 2: 135–145.

Zeng Qingcun (1979), *Mathematical–physical Foundation in Numerical Weather Prediction*, Science Press, pp. 464–471.